MiR-2 family regulates insect metamorphosis by controlling the juvenile hormone signaling pathway

Jesus Lozano[a], Raúl Montañez[a,b], and Xavier Belles[a,1]

[a]Institut de Biologia Evolutiva, Consejo Superior de Investigaciones Científicas, Universitat Pompeu Fabra, 08003 Barcelona, Spain; and [b]Institució Catalana de Recerca i Estudis Avançats–Complex Systems Laboratory, Universitat Pompeu Fabra, 08003 Barcelona, Spain

Edited by Lynn M. Riddiford, Howard Hughes Medical Institute Janelia Farm Research Campus, Ashburn, VA, and approved February 4, 2015 (received for review September 25, 2014)

In 2009 we reported that depletion of Dicer-1, the enzyme that catalyzes the final step of miRNA biosynthesis, prevents metamorphosis in *Blattella germanica*. However, the precise regulatory roles of miRNAs in the process have remained elusive. In the present work, we have observed that Dicer-1 depletion results in an increase of mRNA levels of Krüppel homolog 1 (Kr-h1), a juvenile hormone-dependent transcription factor that represses metamorphosis, and that depletion of Kr-h1 expression in Dicer-1 knockdown individuals rescues metamorphosis. We have also found that the 3′UTR of Kr-h1 mRNA contains a functional binding site for miR-2 family miRNAs (for miR-2, miR-13a, and miR-13b). These data suggest that metamorphosis impairment caused by Dicer-1 and miRNA depletion is due to a deregulation of Kr-h1 expression and that this deregulation is derived from a deficiency of miR-2 miRNAs. We corroborated this by treating the last nymphal instar of *B. germanica* with an miR-2 inhibitor, which impaired metamorphosis, and by treating Dicer-1-depleted individuals with an miR-2 mimic to allow nymphal-to-adult metamorphosis to proceed. Taken together, the data indicate that miR-2 miRNAs scavenge Kr-h1 transcripts when the transition from nymph to adult should be taking place, thus crucially contributing to the correct culmination of metamorphosis.

insect metamorphosis | microRNA | juvenile hormone | evolution of metamorphosis | insect hormones

MicroRNAs (miRNAs) are endogenous, *ca*. 22-nt, single-strand, noncoding RNAs that regulate gene expression by acting posttranscriptionally through basepairing between the so-called seed sequence of the miRNA (nucleotides 2–8 at its 5′ end) and the complementary seed match sequence in the target mRNA (1). Since miRNAs were first discovered in the nematode *Caenorhabditis elegans* in the 1990s (2) and subsequently detected in other species (3), a remarkable diversity of them has been reported in a variety of organisms, including insects, plants, viruses, and vertebrates (4). Information available indicates that miRNAs are key players in gene regulatory networks, driving cell differentiation, conferring robustness, and channeling the development of multicellular organisms (5–8). Furthermore, the escalation in complexity in early bilaterian evolution has been correlated with a strong increase in the number of miRNAs (9–11). In insects, miRNAs have been shown to be involved in fine-tuning a number of biological processes such as cell proliferation, apoptosis and growth, oogenesis, and development, as well as response to biological stress (12).

In 2009 we first looked at whether miRNAs might have a relevant role in the regulation of insect metamorphosis. Only a few published studies had considered the contribution of miRNAs to this process, but these focused on specific aspects, such as wing formation and neuromuscular development (13–16). They also used the fly *Drosophila melanogaster* as a model, a species that follows the holometabolan mode of metamorphosis, in which the juvenile stages are extremely divergent from the adult body plan and thus require a dramatic transformation for adult morphogenesis (17–20). To study the possible role of miRNAs on metamorphosis we used the cockroach *Blattella germanica* as a model, because it displays the more primitive hemimetabolan mode of metamorphosis, where the juvenile stages already have the adult body plan, thus making the transition from nymph to adult much less dramatic than in holometabolan species. In both hemimetabolan and holometabolan modes the regulation of metamorphosis is basically ensured by two hormones, the molting hormone (generally 20-hydroxyecdysone), which triggers nonmetamorphic and metamorphic molts, and the juvenile hormone (JH) that represses the metamorphic character of the molts (21). Our approach involved silencing the expression of Dicer-1, the ribonuclease that produces mature miRNAs from miRNA precursors (22), following a method that had been used successfully in zebrafish (23). The approach was also effective for *B. germanica*, because depletion of Dicer-1 mRNA levels resulted in reduced levels of mature miRNAs and, importantly, prevented metamorphosis; last instar nymphs molted to supernumerary nymphs or to nymph–adult intermediates instead of normal adults (24).

The results obtained for *B. germanica* indicated that miRNAs played a crucial role in regulating metamorphosis, at least in this hemimetabolan model. Our next goal was to unveil which miRNAs and targets were involved, and we started by obtaining a catalog of the miRNAs present in the transition from nymph to adult (25) and then identifying which miRNAs were differentially expressed in this transition; these were let-7, miR-125, and miR-100 (26). A functional study of these miRNAs, however, revealed that they play minor roles in metamorphosis, being related only to wing vein patterning, because depleting them resulted in disorganized vein/intervein patterns and anomalous bifurcations of the wing A-veins (27). Given that none of these

Significance

MicroRNAs are short, single-stranded RNAs that bind to target mRNAs and block their translation. Five years ago we observed in the cockroach *Blattella germanica* that general depletion of microRNAs prevents metamorphosis. This observation led to two key questions: Which microRNAs are involved in this action, and which target do they act on? The results reported herein show that the microRNAs involved are those of an miR-2 family (miR-2, miR-13a, and miR-13b), and the target is the transcription factor Krüppel homolog 1, a master repressor of insect metamorphosis. The data presented indicate that miR-2 microRNAs rapidly clear Krüppel homolog 1 transcripts in the last nymphal instar, a process that is crucial for proper metamorphosis. This reveals the elegant mechanism of an miRNA family leading metamorphosis to its correct conclusion.

Author contributions: J.L., R.M., and X.B. designed research; J.L., R.M., and X.B. performed research; J.L., R.M., and X.B. analyzed data; and J.L. and X.B. wrote the paper.

The authors declare no conflict of interest.

This article is a PNAS Direct Submission.

[1]To whom correspondence should be addressed. Email: xavier.belles@ibe.upf-csic.es.

This article contains supporting information online at www.pnas.org/lookup/suppl/doi:10.1073/pnas.1418522112/-/DCSupplemental.

miRNAs explained the total suppression of metamorphosis observed after depleting Dicer-1 (24), we shifted to an miRNA target approach, choosing Krüppel-homolog 1 (Kr-h1) as a candidate.

Kr-h1 is a JH-dependent transcription factor that represses metamorphosis in both hemimetabolan (28, 29) and holometabolan insects (30, 31) and is a crucial element of the JH signaling pathway comprising Methoprene-tolerant (Met), Kr-h1, and E93, the MEKRE93 pathway (32), which switches metamorphosis on and off in all insects. As in other species, Kr-h1 mRNA is expressed in juvenile instars of *B. germanica* but its expression decreases in the last nymphal instar, when JH titer in the haemolymph also decreases, which is followed by adult morphogenesis (29). RNAi experiments have shown that depleting Kr-h1 in the prelast nymphal instar leads to precocious metamorphosis (29), thus demonstrating the role of master repressor of this transcription factor in adult morphogenesis. An interesting feature of Kr-h1 in *B. germanica* is that the decrease of transcript levels in freshly emerged last nymphal instar is very abrupt (29), a fact that suggested to us the hypothesis that miRNAs could contribute toward modulating it. The work reported herein was addressed to test this hypothesis.

Results and Discussion

Depletion of Dicer-1 Increases Kr-h1 Expression and Depletion of Kr-h1 in Dicer-1 Knockdown Individuals Rescues Metamorphosis. To gain a first insight into whether Kr-h1 might be a promising candidate, we tested whether depletion of Dicer-1, impairing mature miRNA formation, would affect Kr-h1 mRNA levels. We proceeded as in our previous work (24) and treated penultimate instar female nymphs (N5) of *B. germanica* with double-stranded RNA targeting Dicer-1 (dsDicer-1). As expected, Dicer-1 mRNA levels became depleted and mature miRNA levels were reduced (Fig. S1*A*). The dsDicer-1–treated insects ($n = 10$) molted to the next instar nymph (N6) and subsequently to either a perfect supernumerary nymph (N7) (80%) or to nymphoids with membrane-like lateral expansions in the metathorax (20%) (Fig. S1*B*). Two out of the eight N7 insects molted to second supernumerary nymphs (N8) and then to adults, which were bigger than normal and had a blackish abdomen similar in color to that of a nymph (Fig. S1*C*). Control (dsMock-treated) individuals showed normal levels of Dicer-1 mRNA and let-7, and all of them ($n = 10$) molted to N6 and then to normal adults (Fig. S1). Interestingly, mRNA levels of Kr-h1 measured at the beginning of N6 were very low in dsMock-treated animals, as expected, but they were higher in dsDicer-1–treated individuals (Fig. S1*A*). Double dsDicer-1 treatment, one on N5D0 and the other on N5D3, was more efficient in reducing Dicer-1 mRNA levels, and Kr-h1 expression was much higher than in the single dsDicer-1 treatment experiments (Fig. S2*A*); in all cases ($n = 15$), these treatments resulted in perfect supernumerary N7 nymphs that died after molting (Fig. S2*B*).

We then wondered whether Kr-h1 was the main, if not the only, factor affected by miRNA depletion in the context of metamorphosis. Thus, we designed a phenotype rescue experiment by depleting Kr-h1 mRNA levels in Dicer-1 knockdown individuals. Freshly emerged N5s were treated with dsDicer-1 and, just after molting to N6, the same individuals were treated with dsKr-h1. Controls were equivalently treated with dsMock. All individuals treated with dsDicer-1 + dsKr-h1 ($n = 18$) molted to N6 and then to adults, just as the dsMock-treated controls did ($n = 11$) (Fig. 1). The only difference was observed in the membranous hindwings of the individuals treated with dsDicer-1 + dsKr-h1, which were somewhat smaller, wrinkled, and presented defects in the vein/intervein pattern (Fig. 1), reminiscent of the phenotype obtained after depleting let-7, miR-100, and miR-125 (27). As expected, mRNA levels of Kr-h1 were depleted in the individuals treated with dsDicer-1 + dsKr-h1 (Fig. 1). We also measured the expression of the other components of the MEKRE93 pathway, Met and E93, as well as Broad Complex (BR-C), a family of

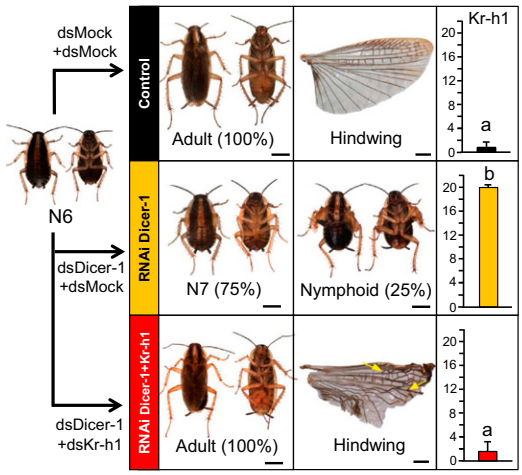

Fig. 1. Effects of Dicer-1 mRNA depletion on Kr-h1 expression and effects of double depletion, of Dicer-1 and Kr-h1, in *B. germanica*. Females freshly ecdysed to the fifth nymphal instar (N5D0) received an injection (3 μg) of dsMock or dsDicer-1. The individuals received a second injection (3 μg) of either dsMock (control) or dsKr-h1 on N6D0. All individuals molted to normal N6. Subsequently, those treated with dsMock + dsMock ($n = 10$) molted to normal adults, with perfect hindwings; Kr-h1 mRNA levels in N6D4 were low. Individuals treated with dsDicer-1 + dsMock ($n = 14$) molted from N6 to perfect supernumerary nymphs (N7) (75%) or nymphoids with membrane-like structures in the metathorax (25%); Kr-h1 mRNA levels in N6D4 were high. Individuals treated with dsDicer-1 + dsKr-h1 ($n = 18$) molted from N6 to normal adults, with imperfect hindwings (smaller, wrinkled, and with defects in the vein/intervein pattern); Kr-h1 mRNA levels in N6D4 were low. Data on Kr-h1 expression represent the mean ± SEM ($n = 4$) and are indicated as copies of Kr-h1 mRNA per 1,000 copies of Actin-5c. The different letters at the top of the columns indicate statistically significant differences (in all cases $P \leq 0.05$), according to the REST software tool. (Scale bars in hindwing, 1 mm and in whole body, 3 mm.)

JH-dependent transcription factors that in postembryonic development of *B. germanica* are involved in wing formation (33). Results showed that transcript levels of Met, which is upstream of Kr-h1, were not affected and those of BR-C were higher than controls in dsDicer-1–treated individuals and returned to normal levels in dsDicer-1 + dsKr-h1–treated individuals; conversely, E93 transcript levels were reduced in dsDicer-1–treated individuals and tended to recover normal levels in the dsDicer-1 + dsKr-h1–treated group (Fig. S2*C*). These results are consistent with the epistatic relationships of these factors in the JH signaling pathway and in the MEKRE93 axis (32). Interestingly, the intermediate levels of E93 expression in dsDicer-1 + dsKr-h1–treated individuals (Fig. S2*C*), associated with low Kr-h1 (Fig. 1) and BR-C (Fig. S2*C*) expression, are sufficient to result in a 100% adult morphogenesis.

Kr-h1 mRNA Contains a Functional Binding Site for miR-2. The above results suggest that inhibition of metamorphosis caused by the absence of mature miRNAs is mainly due to impairing the Kr-h1 mRNA decrease that occurs at the beginning of N6 in *B. germanica*, which would seem to be regulated by miRNAs. To test this hypothesis we started by predicting miRNA binding sites in the 3′UTR of Kr-h1 mRNA using RNAhybrid, miRanda, and PITA algorithms. As queries, we used the miRNAs identified by high-throughput sequencing in *B. germanica* N6 (25). All three algorithms coincided in predicting a top-scored site for miR-2 located at the beginning (nucleotide 67) of the 3′UTR of the Kr-h1 mRNA (Fig. S3*A* and Table S1). In *B. germanica* N6, miR-2 coexists with miR-13a and miR-13b (25), two miRNAs that only differ from miR-2 in 1–3 nt outside the seed region (Fig. S3*B*) and that are predicted to bind at the same miR-2 site on the Kr-h1 mRNA (Table S1). miR-2, miR-13a, and miR-13b have been grouped into the miR-2 family and they cluster together in the genome, which

suggest that they are produced from a single transcript and are coexpressed (34). In the genome of *B. germanica* miR-2, miR-13a, and miR-13b also cluster together (Fig. S3*C*), showing an organization identical to that observed in the flour beetle *Tribolium castaneum*, the silk moth *Bombyx mori*, and the honey bee *Apis mellifera* (34). The cluster also includes miR-71, which do not belong to the miR-2 family but is associated with the same cluster in the same position in these three species and in *B. germanica*.

Interestingly, a top-scored site for miR-2 is also predicted in the 3′UTR of Kr-h1 mRNA of other hemimetabolan insects, such as the linden bug *Pyrrhocoris apterus*, the kissing bug *Rhodnius prolixus*, and the pea aphid *Acyrthosiphon pisum* (Table S1). Conversely, these same algorithms did not predict an miR-2 site in the 3′UTR of Kr-h1 mRNA in holometabolan species, such as *D. melanogaster*, *T. castaneum*, or *B. mori*. In *B. germanica*, the expression pattern of miR-2, miR-13a, and miR-13b in females of the last two nymphal instars, N5 and N6, and the beginning of the adult stage is similar, fluctuating around one copy per copy of U6 (Fig. 2*A*). Intriguingly, these miRNA expression patterns do not correlate with those of Kr-h1 (Fig. 2*A*). A similar fluctuating pattern of miR-2 expression has been observed in the brown plant hopper *Nilaparvata lugens* (35).

To functionally validate the predicted miR-2 binding site we linked the entire Kr-h1 3′UTR containing the miR-2 site to a luciferase reporter gene and expressed this WT construct in *Drosophila* S2 cells. As a negative control, we used the equivalent construct, but linking a Kr-h1 3′UTR version where 8 nt (CUGUGAUA; Fig. S3*A*) of the miR-2 site had been deleted (Mut construct). These 8 nt include those complementary to the seed region of miR-2 miRNAs.

The first measurements revealed that luciferase activity was significantly higher in the Mut construct than in the WT (Fig. 2*B*), owing to the high levels of endogenous miR-2 reported for S2 cells (3, 36). We then determined that miR-2 levels in our S2 cells could be lowered using an miR-2 LNA (locked nucleic acid) inhibitor (miR-2 LNA-i) (Fig. S3*D*). When S2 cells expressing the WT construct were incubated with miR-2 LNA-i, the translation of the construct was derepressed, as indicated by the significant increase in the luciferase signal, as expected. Conversely, the same treatment with miR-2 LNA-i did not modify the luciferase signal in S2 cells expressing the Mut construct (Fig. 2*C*). This suggests that the miR-2 site predicted in the 3′UTR of Kr-h1 mRNA is functional.

We additionally assessed the functionality of this site by treating *B. germanica* in vivo with miR-2 LNA-i (or with miRNA LNA-i Negative Control, for controls) on N6D0 and N6D1 and by measuring miRNA levels on N6D2. The results showed that miR-2 levels were significantly depleted (as were those of miR-13a and miR-13b), whereas those of let-7, used as a negative control, were not (Fig. 2*D*). Kr-h1 mRNA levels were significantly higher than in the controls (Fig. 2*E*), suggesting that miR-2 miRNAs regulate Kr-h1 transcript levels. Interestingly, 1 of the 10 individuals treated with miR-2 LNA-i that was still alive attempted to molt and completed the apolysis but arrested and died without ecdysing. It presented superimposed double cuticular structures, reminiscent of the molting-defective phenotype obtained after depleting the ecdysone receptor (EcR) (37). The new exoskeleton had the general morphology of a supernumerary nymph (N7), and manual removal of the exuvium of the mesonotum and metanotum revealed that there were neither tegmina nor wings developed.

Treatment with an miR-2 Inhibitor Impairs Metamorphosis and Treatment of Dicer-1 Knockdown Individuals with an miR-2 Mimic Restores It. The supernumerary nymph obtained with the miR-2 LNA-i treatment encouraged us to carry out new experiments in vivo following the same approach to study the phenotype. To achieve greater efficiency in the miR-2 depletion, we used a more potent

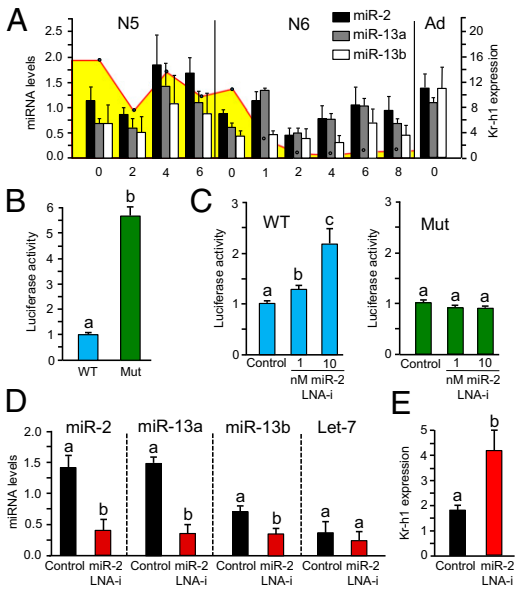

Fig. 2. Expression of miR-2 miRNAs and validation of the miR-2 site in Kr-h1 mRNA of *B. germanica*. (*A*) Expression pattern of miR-2, miR-13a, and miR-13b during N5 and N6, as well as in freshly emerged female adults (Ad); expression of Kr-h1 mRNA levels according to Lozano and Belles (29) is also shown in yellow. (*B*) Luciferase activity in *Drosophila* S2 cells transfected with the construct containing the 3′UTR of Kr-h1 mRNA, and hence containing the miR-2 binding site (WT), and transfected with an equivalent construct with 8 nt of the region that corresponds to the miRNA seed deleted (Mut). (*C*) Luciferase activity in *Drosophila* S2 cells transfected with either the WT or Mut construct, incubated for 48 h with miR-2 miRCURY LNA microRNA Inhibitor (miR-2 LNA-i) or with miRCURY LNA microRNA Inhibitor Negative Control A (control) at a concentration of 0.5 nM; results are expressed as the ratio of *Renilla*/firefly luciferase activity and normalized to the value obtained in the incubations with miRNA LNA-i Negative Control. (*D* and *E*) Effect in vivo of miR-2 LNA-i treatment on miR-2, miR-13a, miR-13b, and let-7 levels (*D*) and Kr-h1 expression (*E*); *B. germanica* female nymphs were treated with 25 nM of miR-2 miRCURY LNA microRNA Inhibitor (miR-2 LNA-i) (or with miRCURY LNA microRNA Inhibitor Negative Control A in the case of controls) on N6D0 and N6D1, and miRNAs or Kr-h1 mRNA levels were quantified on N6D2. In all cases the data represent the mean ± SEM (n = 3–5); miRNA levels are indicated as copies per copy of U6 and Kr-h1 expression is indicated as copies of Kr-h1 mRNA per 1,000 copies of Actin-5c mRNA. The different letters at the top of the columns in each histogram indicate statistically significant differences (in all cases $P \leq 0.05$) according to the REST software tool, or t test in *B* and *C*.

antagonist, namely miR-2 LNA Power Inhibitor (miR-2 LNA-pi), administered in two doses, on N6D0 and N6D1. Controls were equivalently treated with miRNA LNA-i Negative Control. Comparing treated and controls on N6D2 revealed that miR-2 LNA-pi treatment efficiently depleted miR-2 (as well as miR-13a and miR-13b), whereas let-7 was unaffected (Fig. 3*A*). The same samples showed that Kr-h1 mRNA levels were higher in individuals treated with miR-2 LNA-pi than in the controls (Fig. 3*B*), thus indicating that Kr-h1 transcripts had not been properly down-regulated in miR-2–depleted individuals. These results also indicate that miR-2 LNA-pi is more efficient than miR-2 LNA-i in depleting miR-2 miRNAs and derepressing Kr-h1 expression. We additionally carried out equivalent experiments with miR-13a LNA-pi and miR-13b LNA-pi, which showed that both reduced the levels of the three members of the miR-2 family (leaving let-7 levels unaffected), but with less efficiency than that elicited by miR-2 LNA-pi (Fig. S4). In these individuals, Kr-h1 expression was higher than in controls but lower than that observed in miR-2 LNA-pi treatments (compare Fig. 3*A* and Fig. S4). These results show that miR-2 LNA-pi treatment is

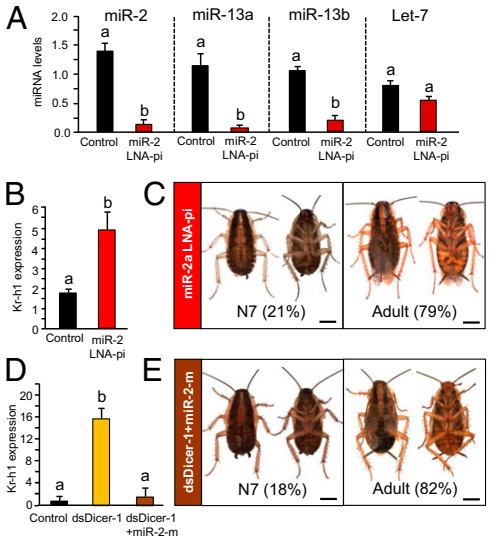

Fig. 3. Effect of miR-2 inhibitor treatment on N6 and of miR-2 mimic treatment of Dicer-1 knockdown individuals of *B. germanica*. (*A*) Effect of miR-2 miRCURY LNA microRNA Power Inhibitor (miR-2 LNA-pi) on miRNA levels; individuals were treated with two doses of 25 nM of miR-2 LNA-pi or miRCURY LNA microRNA Inhibitor Negative Control A (control), one on N6D0 and the other on N6D1, and miRNAs were measured in N6D2. (*B*) Kr-h1 mRNA levels measured in the same samples. (*C*) N7 and adult individuals obtained from miR-2 LNA-pi treatments. (*D*) Effects of dsDicer-1 and miR-2 mimic (miR-2-m) treatments on Kr-h1 transcript levels; dsDicer-1 and dsMock treatments to deplete Dicer-1 mRNA were carried out on N5D0 as described in Fig. 1; the group further treated with miR-2-m received three doses of 25 nM each, on N5D4, N6D0, and N6D1, respectively; the controls of these experiments received an equivalent treatment with miRNA Scramble (controls); Kr-h1 mRNA levels were measured on N6D4. (*E*) N7 and adult individuals obtained from these dsDicer-1 + miR-2 mimic treatments. Data in *A*, *B*, and *D* represent the mean ± SEM ($n = 4$); miRNA levels are indicated as copies per copy of U6 and Kr-h1 expression is indicated as copies of Kr-h1 mRNA per 1,000 copies of Actin-5c mRNA. The different letters at the top of the columns in each histogram indicate statistically significant differences (in all cases $P \leq 0.05$), according to the REST software tool.

the most efficient to simultaneously deplete the three members of the miR-2 family and to impair the down-regulation of Kr-h1 mRNA.

At the phenotypic level, 6 out of 34 miR-2 LNA-pi–treated individuals died shortly after the second treatment. Of the 28 survivors, 6 (21%) molted to supernumerary nymphs (N7) and 22 (79%) molted to normal adults (Fig. 3*C*). These results further suggest that miR-2 miRNAs remove Kr-h1 transcripts at the beginning of the last nymphal instar (N6) of *B. germanica*, thus contributing toward triggering correct metamorphosis. The relatively modest 21% of individuals that did not metamorphose when treated with miR-2 LNA-pi is possibly due to the fact that only this percentage of individuals maintained high-enough Kr-h1 levels to prevent metamorphosis. The treatments with miR-13a LNA-pi and miR-13b LNA-pi ($n = 43$ and 40, respectively) also elicited a modest mortality (5 individuals died in each treatment), and of the 38 and 35 respective survivors, 4 (11%) and 3 (9%) molted to supernumerary nymphs, whereas the remaining individuals molted to normal adults.

Another way to demonstrate that the absence of miR-2 miRNAs in Dicer-1 knockdown individuals is the main explanation for metamorphosis inhibition (24) is through a rescue experiment using an miR-2 mimic. Thus, freshly emerged N5 nymphs were treated with dsDicer-1 and these individuals were then treated with the miR-2 mimic or received an equivalent treatment with miRNA Scramble (controls). Transcript measurements showed that Kr-h1 mRNA levels in dsDicer-1–treated individuals were higher than in the controls, as expected, whereas in those treated with both dsDicer-1 and miR-2 mimic the levels were similar to those observed in the controls (Fig. 3*D*). At the phenotypic level, the individuals treated with both dsMock and miRNA Scramble ($n = 10$) molted to N6 and then to normal adults, and those treated with dsDicer-1 + miRNA Scramble ($n = 10$) molted to N6 and then to N7. In the group of individuals treated with both dsDicer-1 + miR-2 mimic ($n = 33$), 6 (18%) molted to N6 and then to N7, whereas the remaining 21 individuals molted to N6 and then to adults (Fig. 3*E*). These adults presented a normal morphology except for the occurrence of small defects in the vein/intervein pattern in the membranous hindwings (Fig. S5*A*). These defects are reminiscent of those observed in the dsDicer-1 + dsKr-h1 treatments described above (Fig. 1) and in individuals that were depleted for let-7, miR-100, and miR-125 in N6 (27).

As expected, miR-2 levels were very high in the individuals treated with dsDicer-1 + miR-2 mimic, whereas those of let-7 were unaffected (Fig. S5*B*). The levels of miR-13a and miR-13b were also unaffected (Fig. S5*B*), which indicates that the primers used to measure miR-13a and miR-13b do not measure miR-2, which additionally suggests that the primers used to measure the three members of the miR-2 family (as in Fig. 2*A*) are specific. Transcript levels of Met were not modified by the treatments of dsDicer-1 + miR-2 mimic, and those of BR-C were higher than controls in dsDicer-1–treated individuals and returned to normal levels in dsDicer-1 + miR-2 mimic-treated individuals. Conversely, E93 expression was reduced in dsDicer-1–treated individuals and tended to recover normal levels in dsDicer-1 + miR-2 mimic-treated individuals (Fig. S5*B*). Interestingly, these results parallel those obtained with the treatments of dsDicer-1 + dsKr-h1 (Fig. 1), which rescued 100% normal metamorphosis. In this case the rescue was not complete (82% of individuals molted to the adult stage), which is possibly associated with the still-low average levels of recovery of E93 expression after miR-2 mimic treatment.

An miRNA Family That Leads Metamorphosis to a Correct Conclusion. We had observed in *B. germanica* that depletion of Dicer-1 and consequent reduction of miRNA levels prevented metamorphosis (24). The results presented herein show that Dicer-1 depletion results in increased levels of Kr-h1 mRNA, and that RNAi of Kr-h1 in Dicer-1 knockdown individuals rescues metamorphosis. Both results suggest that the inhibition of metamorphosis caused by miRNA depletion is due to a deregulation of Kr-h1 expression. Moreover, the 3′UTR of Kr-h1 mRNA contains a functional binding site for miR-2 miRNAs, suggesting that the deregulation of Kr-h1 might be due to a deficiency of miR-2 and their variants, miR-13a and miR-13b. We have corroborated this by treating N6 of *B. germanica* with an miR-2 inhibitor, impairing metamorphosis, and by treating Dicer-1–depleted individuals with an miR-2 mimic, which restored metamorphosis. Taken together, the data indicate that miR-2 miRNAs modulate Kr-h1 mRNA levels and that this is crucial for metamorphosis.

Recent studies have shown that the transcription factor Met is the JH receptor and that downstream of Met the JH signal is transduced by Kr-h1 (38). In prefinal stages, Kr-h1 exerts its antimetamorphic action by repressing E93 (32), a transcription factor that triggers adult morphogenesis (32, 39). Thus, the Met–Kr-h1–E93 axis, or the MEKRE93 pathway (32), switches adult morphogenesis on and off, as observed, among other models, in *B. germanica* (29, 32, 39, 40). Kr-h1 is expressed in juvenile instars, but its expression abruptly decreases at the beginning of N6 (29), coinciding with the gradual decrease of JH levels in the hemolymph (41). Treatment with JH reinduces Kr-h1 expression and inhibits adult morphogenesis, indicating that the decrease in Kr-h1 expression at the beginning of N6 is crucial for metamorphosis and that it is primarily triggered by the decrease of JH levels (29). However, the decrease of Kr-h1 mRNA levels is very abrupt, which suggests that there are additional mechanisms

regulating it, one of these being the repression exerted by E93 on Kr-h1 expression (32, 39). This led us to wonder whether this repressive action is mediated by miR-2, and to test whether E93 stimulates the expression of miR-2 using E93-depleted individuals as in previous experiments (32). miR-2 levels in these individuals were very similar to those of respective controls (Fig. S6), which suggests that the antagonistic actions of E93 and miR-2 over Kr-h1 expression are independent. Therefore, miR-2 miRNAs seem to play a role of Kr-h1 transcript scavenger in a precise developmental stage that is of paramount importance for correct metamorphosis. This would lead us to expect that the respective expression patterns should inversely correlate. However, this is not the case (Fig. 2*A*), possibly because miR-2 miRNAs regulate multiple targets (42), as well as the fact that Kr-h1 expression is constantly enhanced while JH is present, and it is only at the beginning of N6, when JH vanishes, that there is full, efficient depletion of the Kr-h1 transcripts.

The presence of an miR-2 binding site in the 3′UTR of Kr-h1 mRNA of hemipterans (Table S1), and the observation that the expression pattern of Kr-h1 in hemipterans (28) and ephemeropterans (43) also decreases at the beginning of the preadult stage, suggest that the clearing of Kr-h1 transcripts by miR-2 miRNAs, thus allowing correct metamorphosis, is a common mechanism in hemimetabolan species. In contrast, we were not able to identify miR-2 sites in the Kr-h1 mRNA of holometabolan species, indicating that the above inhibitory mechanism of miR-2 upon Kr-h1 has been lost in the evolutionary transition from hemimetaboly to holometaboly. Indeed, RNAi of Dicer-1 in *T. castaneum* only results in occasional wing expansion defects (44), suggesting that in holometabolan species miRNAs only play refining roles in particular morphogenetic processes, such as wing formation. A number of reports support this hypothesis; for example, during adult morphogenesis of *D. melanogaster*, let-7 is required for neuromusculature remodeling (16), whereas let-7 and miR-125 are needed for proper timing in the wing cell cycle and for the maturation of neuromuscular junctions (14). Also in *D. melanogaster*, iab-4 attenuates Ultrabithorax expression and causes a transformation of halteres to wings (15), whereas miR-9a contributes to wing development by modulating the expression of the transcription factor dLMO, which represses Apterous, a factor required for the proper dorsal identity of the wings (13). Specific miRNA functions in wing development have also been described in hemimetabolan species such as *B. germanica*, where depletion of let-7 and associated miRNAs affects vein patterning (27). Thus, we presume that the contribution of miRNAs to wing development is an ancestral function in insects, which perhaps originated with the first pterygotes, some 350 million y ago (45, 46).

The concept emerging is that a single miRNA family leads metamorphosis to its correct conclusion. This is reminiscent of the role of a single miRNA, the cell's Nepenthe, that removes maternal transcripts during the maternal-to-zygotic transition (47) to allow a new life to start. In this case the miR-2 miRNAs clear away a single transcript that is preventing the transition to the adult stage—a stage that, in some ways, also represents a new life.

Materials and Methods

Insects. Individuals of *B. germanica* were obtained from a colony reared in the dark at 30 ± 1 °C and 60–70% relative humidity. Freshly ecdysed female nymphs were selected and used at the appropriate ages. They were anesthetized with carbon dioxide before injection treatments, dissections, and tissue sampling.

RNA Extraction and Retrotranscription to cDNA. We performed total RNA extraction from the whole body, using the miRNeasy extraction kit (Qiagen). For mRNA quantification a 500-ng sample from each RNA extraction was treated with DNase (Promega) and reverse-transcribed with SuperScript II reverse transcriptase (Invitrogen) and random hexamers (Promega). RNA quantity and quality was estimated by spectrophotometric absorption at 260 nm using a Nanodrop Spectrophotometer ND-1000 (NanoDrop Technologies). For miRNA quantification an amount of 500 ng of total RNA was reverse-transcribed with the NCodeTM miRNA first-strand synthesis and qRT-PCR kit (Invitrogen), following the manufacturer's protocol. All PCR products were subcloned into the pSTBlue-1 vector (Novagen) and sequenced.

Quantification of miRNAs and mRNAs by Quantitative Real-Time PCR. Quantitative real-time PCR (qRT-PCR) reactions were performed in triplicate in an iQ5 Real-Time PCR Detection System (Bio-Rad Laboratories), using SYBRGreen (Power SYBR Green PCR Master Mix; Applied Biosystems). A template-free control was included in all batches. Primer efficiency was first validated by constructing a standard curve through four serial dilutions and was assessed using the Bio-Rad iQ5 Standard Edition Optical System Software (version 2.0). mRNA levels were calculated relative to BgActin-5c (Accession no. AJ862721) expression. Results are given as copies of mRNA per 1,000 copies of BgActin-5c mRNA. Primers are described in Table S2. In the case of miRNAs, we used the U6 from *B. germanica* (accession no. FR823379) as a reference, and thus results are given as copies of RNA per copies of U6 (25). miRNA primers are also described in Table S2. Given the structural similarity of miR-2, miR-13a, and miR13b, we carefully assessed the specificity of the respective primers by confirming that the melting curve corresponding to each amplification presented a single peak and that the three respective melting temperatures were different.

RNAi. The detailed procedures for RNAi have been reported previously (24). Primers to prepare the dsRNAs are described in Table S2. The sequences were amplified by PCR and cloned into the pSTBlue-1 vector. A 307-bp sequence from *Autographa californica* nucleopolyhedrosis virus (Accession no. K01149, from nucleotides 370–676) was used as control dsRNA (dsMock). A volume of 1 μL of the respective dsRNA solution (3 μg/μL) was injected into the abdomen of individuals at chosen stages.

Prediction of miRNA Binding Sites. To predict binding sites in the 3′UTR of Kr-h, we used the following three algorithms and parameter sets. RNAhybrid (bibiserv.techfak.uni-bielefeld.de/rnahybrid/) (48), with a distribution probability of parameter $\xi = 1.98$ and $\theta = 1.16$; miRanda (www.microrna.org/microrna/) (49), with a score threshold of 134; and PITA (genie.weizmann.ac.il/index.html) (50), with the seed limitation between 5 and 8 and with Firefly luciferase as a 5′ upstream.

Luciferase Assay to Assess the Effect of miR-2 on the mRNA of Kr-h1. Two reporter constructs were generated by cloning downstream of Firefly luciferase coding region, under the control of an Ac5 promoter, a WT or a mutated (Mut) 3′-UTR of *B. germanica* Kr-h1. WT 3′-UTR was generated by PCR amplification from a pSTBlue-1 vector (Novagen) with the Kr-h1 transcript, using the primers described in Table S2. To generate the Mut version, a directed site mutagenesis was carried out to remove the 8 nt of the 3′ end of the site (CUGUGAUA; Fig. S3*A*), which include the region complementary to the miR-2 seed, taking the WT vector as template and using the primers described in Table S2. We modified the plasmid pAc5.1 and inserted a Firefly luciferase coding region in KpnI site and NotI and under the control of the Ac5 promoter. Then, we added a new multicloning site from pStBlue. Kr-h1 3′UTR was finally cloned downstream of the Firefly luciferase coding region of plasmid pAc5 + Luciferase. All PCR fragments were cloned in the pAc5 vector and confirmed by sequencing. To perform the luciferase essay, S2 cells were transfected in 24-well plates with Insect GeneJuice (Novagen) following the manufacturer's instructions. Transfection was performed in triplicate with the following mixture per well: 500 ng of Firefly luciferase reporter plasmid, WT or Mut, and 500 ng of the *Renilla* luciferase, as a transfection control plasmid. In the experiments with miR-2 antagonists, miR-2 LNA-i (or miRNA LNA-i Negative Control for controls) was added at a concentration of 0.5 nM. After 48 h of transfection, Dual-Glo luciferase assays (Promega) were performed following the manufacturer's instructions and measured in an Orion II microplate luminometer (Titertek-Berthold). Results are expressed as the ratio of *Renilla*/firefly luciferase activity (mean ± SEM) based on three to five independent replicates and normalized to the value obtained in the incubations with miRNA LNA-i Negative Control.

Experiments with miRNA Inhibitors and miRNA Mimics. To deplete miR-2 in the experiments for validating the miRNA binding site, miR-2 miRCURY LNA microRNA Inhibitor (miR-2 LNA-i) (Exiqon) was used. In the experiments to inhibit metamorphosis, miR-2a miRCURY LNA microRNA Power Inhibitor (miR-2 LNA-pi) (Exiqon), which has more powerful action and resistance against DNases, was used. miRCURY LNA microRNA Inhibitor Negative Control A (Exiqon) was used as control. In all experiments individuals were treated with two doses of 25 nM each of inhibitor or negative control, one on N6D0 and the other on N6D1, and effects were determined on N6D2. To rescue metamorphosis in Dicer-1–depleted individuals, GMR-miR microRNA double-stranded mimics from GenePharma (51) (miR-2a mimic and miRNA

Scramble as negative control) were used. Individuals that had been treated with dsDicer-1 in N5D0 were treated with three doses of 25 nM each of the miR-2 mimic or the corresponding control in N5D4, N6D0, and N6D1, and results in terms of transcript measurements were studied on N6D4.

Statistical Analysis. Significance of the differences between treated and control samples was determined with the REST software tool (52).

ACKNOWLEDGMENTS. We thank Carolina G. Santos for providing samples of *B. germanica* E93 knockdown individuals and Guillem Ylla for searching miRNA genes in the *B. germanica* genome, which is available at https://www.hgsc.bcm.edu/arthropods/german-cockroach-genome-project, as provided by the Baylor College of Medicine Human Genome Sequencing Center. This work was supported by Ministerio de Ciencia e Innovación Grant CGL2008-03517/BOS (to X.B.); Ministerio de Economía y Competitividad Grant CGL2012-36251 (to X.B.); a predoctoral fellowship (to J.L.), by Catalan Government Grant 2014 SGR 619; and by the Consejo Superior de Investigaciones Cientificas (a postdoctoral contract to R.M. from the Junta para la Ampliación de Estudios program). The research has also benefited from Fonds Européen de Développement Régional.

1. Bartel DP (2004) MicroRNAs: Genomics, biogenesis, mechanism, and function. *Cell* 116(2):281–297.
2. Lee RC, Feinbaum RL, Ambros V (1993) The *C. elegans* heterochronic gene lin-4 encodes small RNAs with antisense complementarity to lin-14. *Cell* 75(5):843–854.
3. Lagos-Quintana M, Rauhut R, Lendeckel W, Tuschl T (2001) Identification of novel genes coding for small expressed RNAs. *Science* 294(5543):853–858.
4. Griffiths-Jones S, Grocock RJ, van Dongen S, Bateman A, Enright AJ (2006) miRBase: MicroRNA sequences, targets and gene nomenclature. *Nucleic Acids Res* 34(Database issue):D140–D144.
5. Hornstein E, Shomron N (2006) Canalization of development by microRNAs. *Nat Genet* 38(Suppl):S20–S24.
6. Ivey KN, Srivastava D (2010) MicroRNAs as regulators of differentiation and cell fate decisions. *Cell Stem Cell* 7(1):36–41.
7. Kloosterman WP, Plasterk RH (2006) The diverse functions of microRNAs in animal development and disease. *Dev Cell* 11(4):441–450.
8. Shomron N (2010) MicroRNAs and developmental robustness: A new layer is revealed. *PLoS Biol* 8(6):e1000397.
9. Christodoulou F, et al. (2010) Ancient animal microRNAs and the evolution of tissue identity. *Nature* 463(7284):1084–1088.
10. Grimson A, et al. (2008) Early origins and evolution of microRNAs and Piwi-interacting RNAs in animals. *Nature* 455(7217):1193–1197.
11. Wheeler BM, et al. (2009) The deep evolution of metazoan microRNAs. *Evol Dev* 11(1):50–68.
12. Belles X, Cristino AS, Tanaka ED, Rubio M, Piulachs M-D (2012) Insect microRNAs: From molecular mechanisms to biological roles. *Insect Molecular Biology and Biochemistry*, ed Gilbert LI (Elsevier, Amsterdam), pp 30–56.
13. Biryukova I, Asmar J, Abdesselem H, Heitzler P (2009) Drosophila mir-9a regulates wing development via fine-tuning expression of the LIM only factor, dLMO. *Dev Biol* 327(2):487–496.
14. Caygill EE, Johnston LA (2008) Temporal regulation of metamorphic processes in Drosophila by the let-7 and miR-125 heterochronic microRNAs. *Curr Biol* 18(13):943–950.
15. Ronshaugen M, Biemar F, Piel J, Levine M, Lai EC (2005) The Drosophila microRNA iab-4 causes a dominant homeotic transformation of halteres to wings. *Genes Dev* 19(24):2947–2952.
16. Sokol NS, Xu P, Jan YN, Ambros V (2008) Drosophila let-7 microRNA is required for remodeling of the neuromusculature during metamorphosis. *Genes Dev* 22(12):1591–1596.
17. Belles X (2011) Origin and evolution of insect metamorphosis. *Encyclopedia of Life Sciences* (Wiley, Chichester, UK).
18. Truman JW, Riddiford LM (1999) The origins of insect metamorphosis. *Nature* 401(6752):447–452.
19. Truman JW, Riddiford LM (2002) Endocrine insights into the evolution of metamorphosis in insects. *Annu Rev Entomol* 47:467–500.
20. Sehnal F, Svacha P, Zrzavy J (1996) Evolution of insect metamorphosis. *Metamorphosis*, eds Gilbert LI, Tata JR, Atkinson BG (Elsevier, Amsterdam), pp 3–58.
21. Nijhout HF (1994) *Insect Hormones* (Princeton Univ Press, Princeton).
22. Lee YS, et al. (2004) Distinct roles for Drosophila Dicer-1 and Dicer-2 in the siRNA/miRNA silencing pathways. *Cell* 117(1):69–81.
23. Giraldez AJ, et al. (2005) MicroRNAs regulate brain morphogenesis in zebrafish. *Science* 308(5723):833–838.
24. Gomez-Orte E, Belles X (2009) MicroRNA-dependent metamorphosis in hemimetabolan insects. *Proc Natl Acad Sci USA* 106(51):21678–21682.
25. Cristino AS, Tanaka ED, Rubio M, Piulachs MD, Belles X (2011) Deep sequencing of organ- and stage-specific microRNAs in the evolutionarily basal insect *Blattella germanica* (L.) (Dictyoptera, Blattellidae). *PLoS ONE* 6(4):e19350.
26. Rubio M, de Horna A, Belles X (2012) MicroRNAs in metamorphic and non-metamorphic transitions in hemimetabolan insect metamorphosis. *BMC Genomics* 13:386.
27. Rubio M, Belles X (2013) Subtle roles of microRNAs let-7, miR-100 and miR-125 on wing morphogenesis in hemimetabolan metamorphosis. *J Insect Physiol* 59(11):1089–1094.
28. Konopova B, Smykal V, Jindra M (2011) Common and distinct roles of juvenile hormone signaling genes in metamorphosis of holometabolous and hemimetabolous insects. *PLoS ONE* 6(12):e28728.
29. Lozano J, Belles X (2011) Conserved repressive function of Krüppel homolog 1 on insect metamorphosis in hemimetabolous and holometabolous species. *Sci Rep* 1:163.
30. Minakuchi C, Namiki T, Shinoda T (2009) Krüppel homolog 1, an early juvenile hormone-response gene downstream of Methoprene-tolerant, mediates its anti-metamorphic action in the red flour beetle *Tribolium castaneum*. *Dev Biol* 325(2):341–350.
31. Minakuchi C, Zhou X, Riddiford LM (2008) Krüppel homolog 1 (Kr-h1) mediates juvenile hormone action during metamorphosis of *Drosophila melanogaster*. *Mech Dev* 125(1–2):91–105.
32. Belles X, Santos CG (2014) The MEKRE93 (Methoprene tolerant-Krüppel homolog 1-E93) pathway in the regulation of insect metamorphosis, and the homology of the pupal stage. *Insect Biochem Mol Biol* 52:60–68.
33. Huang JH, Lozano J, Belles X (2013) Broad-complex functions in postembryonic development of the cockroach *Blattella germanica* shed new light on the evolution of insect metamorphosis. *Biochim Biophys Acta* 1830(1):2178–2187.
34. Marco A, Hooks K, Griffiths-Jones S (2012) Evolution and function of the extended miR-2 microRNA family. *RNA Biol* 9(3):242–248.
35. Chen J, Liang Z, Liang Y, Pang R, Zhang W (2013) Conserved microRNAs miR-8-5p and miR-2a-3p modulate chitin biosynthesis in response to 20-hydroxyecdysone signaling in the brown planthopper, *Nilaparvata lugens*. *Insect Biochem Mol Biol* 43(9):839–848.
36. Moretti F, Kaiser C, Zdanowicz-Specht A, Hentze MW (2012) PABP and the poly(A) tail augment microRNA repression by facilitated miRISC binding. *Nat Struct Mol Biol* 19(6):603–608.
37. Cruz J, Mané-Padrós D, Bellés X, Martín D (2006) Functions of the ecdysone receptor isoform-A in the hemimetabolous insect *Blattella germanica* revealed by systemic RNAi in vivo. *Dev Biol* 297(1):158–171.
38. Jindra M, Palli SR, Riddiford LM (2013) The juvenile hormone signaling pathway in insect development. *Annu Rev Entomol* 58:181–204.
39. Ureña E, Manjón C, Franch-Marro X, Martín D (2014) Transcription factor E93 specifies adult metamorphosis in hemimetabolous and holometabolous insects. *Proc Natl Acad Sci USA* 111(19):7024–7029.
40. Lozano J, Belles X (2014) Role of Methoprene-tolerant (Met) in adult morphogenesis and in adult ecdysis of *Blattella germanica*. *PLoS ONE* 9(7):e103614.
41. Treiblmayr K, Pascual N, Piulachs MD, Keller T, Belles X (2006) Juvenile hormone titer versus juvenile hormone synthesis in female nymphs and adults of the German cockroach, *Blattella germanica*. *J Insect Sci* 6:1–7.
42. Stark A, Brennecke J, Russell RB, Cohen SM (2003) Identification of Drosophila microRNA targets. *PLoS Biol* 1(3):E60.
43. Minakuchi C, Tanaka M, Miura K, Tanaka T (2011) Developmental profile and hormonal regulation of the transcription factors broad and Krüppel homolog 1 in hemimetabolous thrips. *Insect Biochem Mol Biol* 41(2):125–134.
44. Tomoyasu Y, et al. (2008) Exploring systemic RNA interference in insects: A genome-wide survey for RNAi genes in Tribolium. *Genome Biol* 9(1):R10.
45. Grimaldi D, Engel MS (2005) *Evolution of the Insects* (Cambridge Univ Press, Cambridge, UK).
46. Heming BS (2003) *Insect Development and Evolution* (Comstock, Ithaca, NY).
47. Giraldez AJ (2010) MicroRNAs, the cell's Nepenthe: Clearing the past during the maternal-to-zygotic transition and cellular reprogramming. *Curr Opin Genet Dev* 20(4):369–375.
48. Rehmsmeier M, Steffen P, Hochsmann M, Giegerich R (2004) Fast and effective prediction of microRNA/target duplexes. *RNA* 10(10):1507–1517.
49. Enright AJ, et al. (2003) MicroRNA targets in *Drosophila*. *Genome Biol* 5(1):R1.
50. Kertesz M, Iovino N, Unnerstall U, Gaul U, Segal E (2007) The role of site accessibility in microRNA target recognition. *Nat Genet* 39(10):1278–1284.
51. Thomson DW, Bracken CP, Szubert JM, Goodall GJ (2013) On measuring miRNAs after transient transfection of mimics or antisense inhibitors. *PLoS ONE* 8(1):e55214.
52. Pfaffl MW, Horgan GW, Dempfle L (2002) Relative expression software tool (REST) for group-wise comparison and statistical analysis of relative expression results in real-time PCR. *Nucleic Acids Res* 30(9):e36.

Supporting Information

Lozano et al. 10.1073/pnas.1418522112

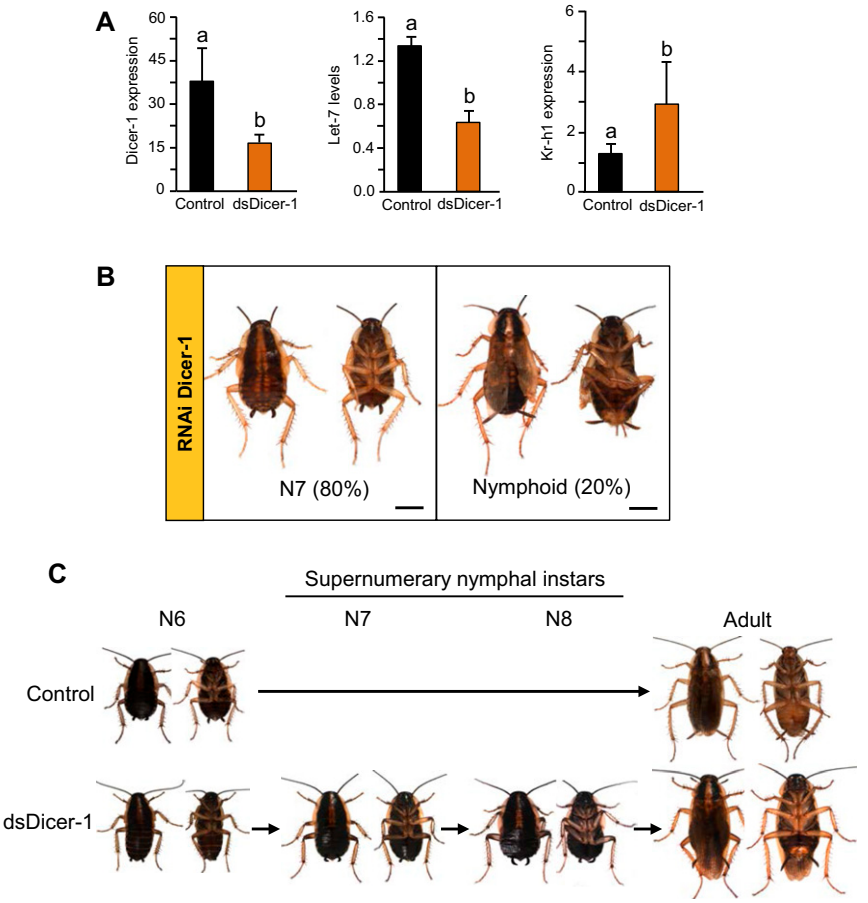

Fig. S1. Effects of Dicer-1 depletion in *Blattella germanica*. Females freshly ecdysed to the fifth nymphal instar (N5D0) received an injection (3 μg) of dsMock or dsDicer-1. (*A*) The levels of Dicer-1 mRNA and let-7 on N6D2 were significantly lower than in the controls, whereas Kr-h1 mRNA levels were higher; data represent the mean ± SEM ($n = 4$), Dicer-1 and Kr-h1 expression is indicated as copies of the respective mRNA per 1,000 copies of Actin-5c, and let-7 levels are indicated as copies of let-7 per copy of U6; the different letters at the top of the columns in each histogram indicate statistically significant differences (in all cases $P \leq 0.05$), according to the REST software tool. (*B*) Experimental individuals molted to normal N6 in all cases; subsequently, dsMock-treated individuals ($n = 10$) molted from N6 to normal adults, whereas dsDicer-1–treated individuals ($n = 10$) molted from N6 to perfect supernumerary nymphs (N7) (80%) or to nymphoids with membrane-like lateral expansions in the metathorax (20%). (*C*) Two out of eight of the perfect N7 obtained from dsDicer-1 treatments molted to a second morphologically perfect supernumerary nymph (N8), and then to adults that were bigger than normal and presented a blackish abdomen, similar in color to that of a nymph.

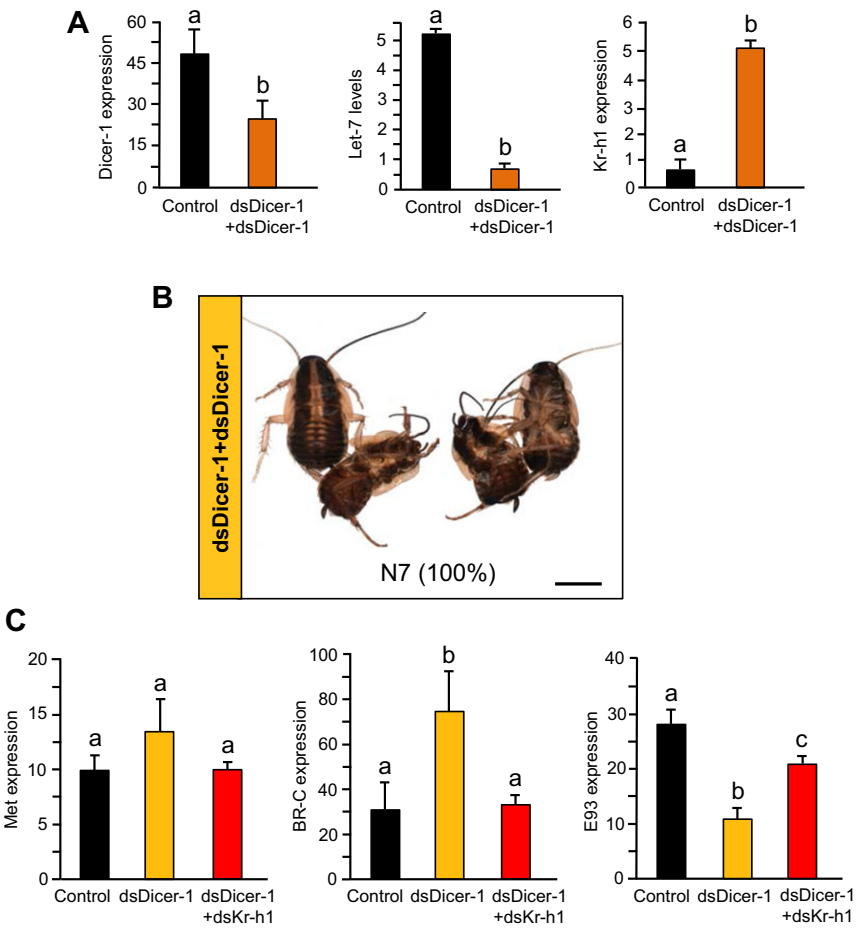

Fig. S2. Effects of dsDicer-1 and dsKr-h1 in *B. germanica*. (*A* and *B*) Effects of double treatment with dsDicer-1. Females received two 3-μg injections of dsMock or dsDicer-1, one when freshly ecdysed to the fifth nymphal instar (N5D0) and the other on N5D3. (*A*) Levels of Dicer-1 mRNA and let-7 on N6D2 were significantly lower than in the controls, whereas Kr-h1 mRNA levels were dramatically higher. (*B*) In each case, all experimental individuals molted to normal N6, and then to N7 (100%); however, they died during ecdysis, being unable to detach from the exuvium. (*C*) Effects of dsDicer-1 on Kr-h1 expression and of double RNAi, with dsDicer-1 and dsKr-h1on the expression of transcription factors Methoprene-tolerant (Met), Broad-complex (BR-C), and E93. Females freshly ecdysed to fifth nymphal instar (N5D0) received an injection (3 μg) of dsMock or dsDicer-1. The same individuals received a second injection (3 μg) either of dsMock (Control) or dsKr-h1 on N6D0. In *A* and *C*, data represent the mean ± SEM ($n = 4$); Dicer-1, Kr-h1, Met, BR-C, and E93 expression is indicated as copies of the respective mRNA per 1,000 copies of Actin-5c mRNA, whereas let-7 levels are indicated as copies of let-7 per copy of U6. The different letters at the top of the columns in each histogram indicate statistically significant differences (in all cases $P \leq 0.05$), according to the REST software tool.

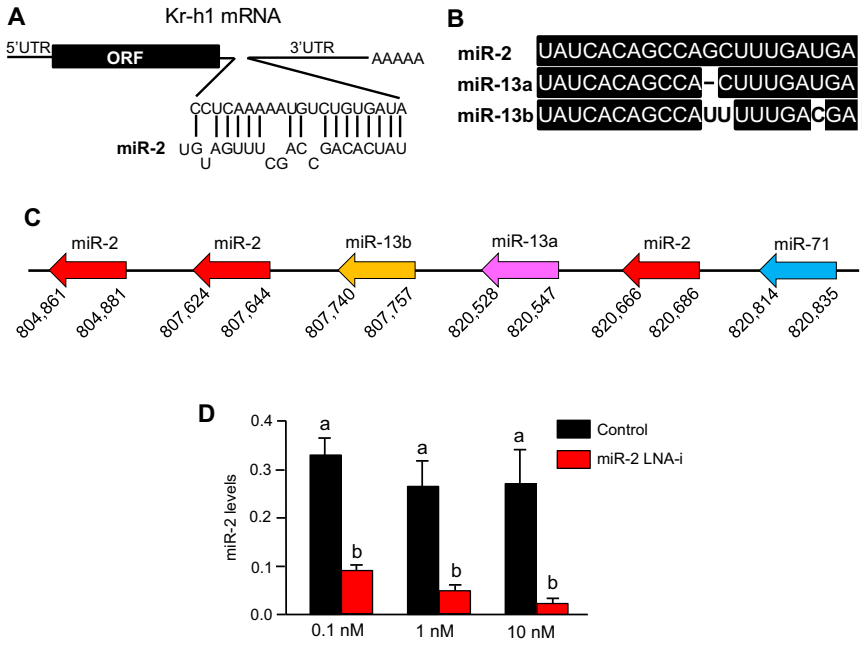

Fig. S3. miR-2 binding site, miR-2 family in *B. germanica*, and effects of miR-2 LNA inhibitor in vitro. (*A*) Schematic representation of Kr-h1 mRNA showing the predicted miR-2 binding site at nucleotide 67 on the 3′UTR. (*B*) Alignment of the three members of the miR-2 family found in the last nymphal instar (N6) of *B. germanica*. (*C*) Genomic organization of mir-2 family sequences; the three miRNAs are found in the scaffold 804 of the *B. germanica* genome version 1.0 (GenBank assembly ID: GCA_000762945.1) (see https://www.hgsc.bcm.edu/arthropods/german-cockroach-genome-project). Identical organization is observed in *Tribolium castaneum*, *Bombyx mori*, and *Apis mellifera* (1). The blue arrow depicts mir-71, which does not belong to miR-2 family but is associated to the same cluster in the same position in these three species and in *B. germanica*. Distances between arrows are not proportional to real length. The numbers indicate the position of each mature miRNA in scaffold 804. (*D*) Effect of an miR-2 LNA inhibitor (miR-2 LNA-i) on levels of miR-2 in *Drosophila* S2 cells incubated in vitro. Control cells were treated with Scramble LNA. Measurements were performed after 48 h of incubation; data represent the mean ± SEM (n = 3–5); miRNA levels are indicated as copies per copy of U6. The different letters at the top of the columns indicate statistically significant differences (in all cases $P \leq 0.05$), according to the REST software tool.

1. Marco A, Hooks K, Griffiths-Jones S (2012) Evolution and function of the extended miR-2 microRNA family. *RNA Biol* 9(3):242–248.

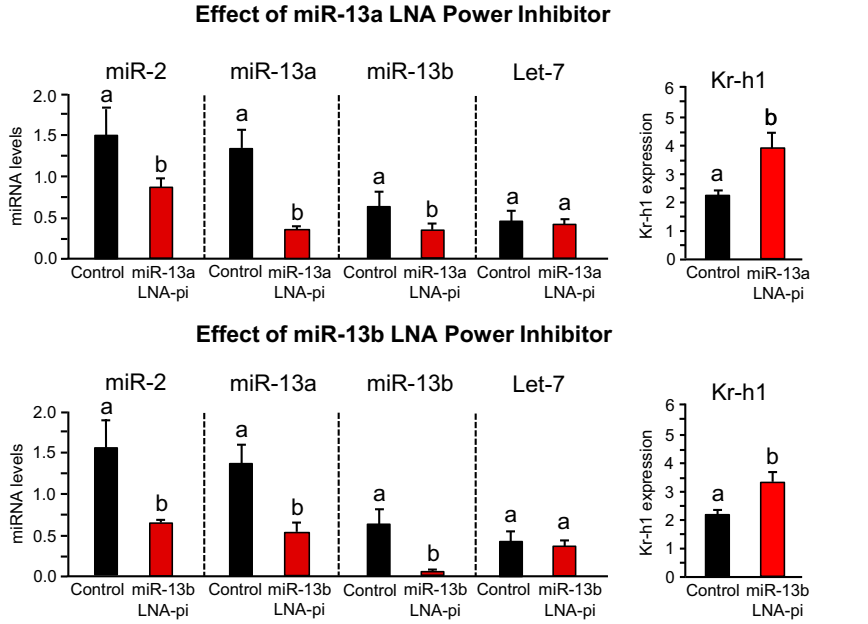

Fig. S4. Effect of miR-13a and miR13b LNA Power Inhibitor (miR-13a LNA-pi and miR-13b LNA-pi) on miRNA levels in *B. germanica*. Individuals were treated with two doses of 25 nM each of the corresponding LNA-pi or of miRNA Inhibitor Negative Control (Control), one on N6D0 and the other on N6D1. Kr-h1 expression and miRNA levels were measured in N6D2; miRNA levels are indicated as copies of the respective miRNA per copy of U6; Kr-h1 expression is indicated as copies of Kr-h1 mRNA per 1,000 copies of Actin-5c mRNA; data represent the mean ± SEM (n = 4). The different letters at the top of the columns in each histogram indicate statistically significant differences (in all cases $P \leq 0.05$), according to the REST software tool.

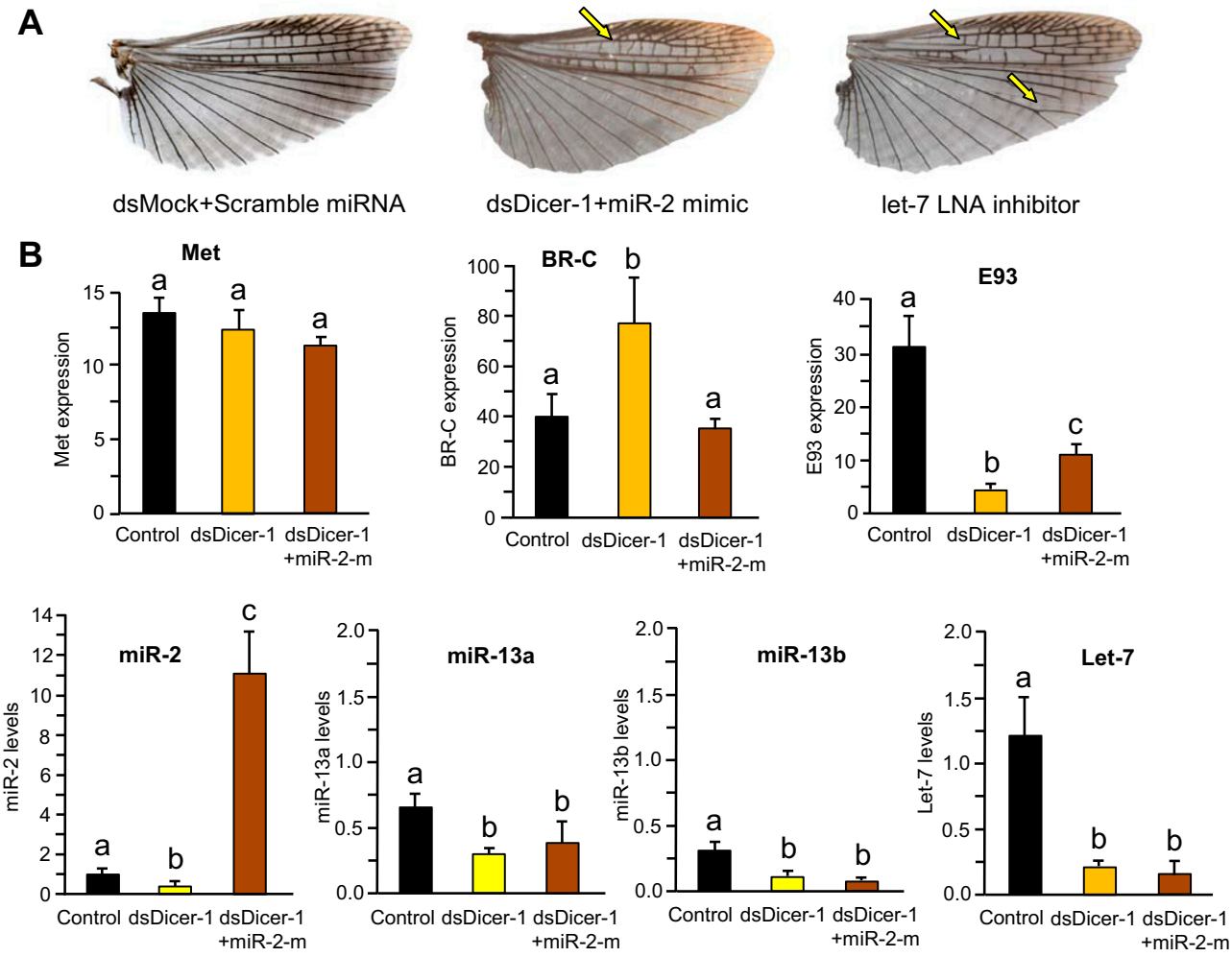

Fig. S5. Effects of miR-2 mimic (miR-2-m) treatment on Dicer-1–depleted individuals of *B. germanica*. Females freshly ecdysed to fifth nymphal instar (N5D0) received an injection (3 μg) of dsMock or dsDicer-1; the group further received three doses of 25 nM each of miR-2-m, on N5D4, N6D0, and N6D1; controls received an equivalent treatment with miRNA mimic Scramble (Controls). (*A*). Adult female hindwings from a control individual treated with dsMock + Scramble miRNA, from a individual treated with dsDicer-1 + miR-2 mimic (note the disorganized vein/intervein pattern in the anterior wing region shown by the arrow), and from a individual treated with let-7 LNA inhibitor (data and image are from ref. 1); note that the wing show defects in the vein/intervein patterning in the anterior wing region, as well as anomalous vein bifurcation in the posterior wing region: arrows). (*B*) Effects of miR-2-m treatment on Dicer-1–depleted individuals upon mRNA levels of Methoprene-tolerant (Met), Broad-complex (BR-C), and E93, as well as on levels of miR-2, miR-13a, miR-13b, and let-7, measured on N6D4. Data represent the mean ± SEM ($n = 4$). Expression of Met, BR-C and E93 is indicated as copies of mRNA per 1,000 copies of Actin-5c mRNA; miR-2, miR-13a, miR-13b, and let-7 levels are indicated as copies of miRNA per copy of U6. The different letters at the top of the columns indicate statistically significant differences comparing treatments ($P \leq 0.05$), according to the REST software tool.

1. Rubio M, Belles X (2013) Subtle roles of microRNAs let-7, miR-100 and miR-125 on wing morphogenesis in hemimetabolan metamorphosis. *J Insect Physiol* 59(11):1089–1094.

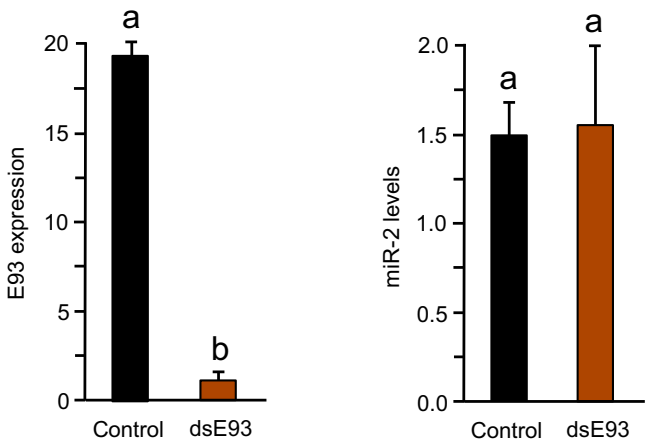

Fig. S6. Effects of E93 depletion on miR-2 expression levels in *B. germanica*. RNA extracts were from E93-depleted individuals, and the respective controls (dsMock-treated), obtained by Belles and Santos (1). Males freshly ecdysed to fifth nymphal instar (N5D0) received an injection (2 μg) of dsMock or dsE93 and were dissected on N6D4. Data represents the mean ± SEM ($n = 4$). E93 expression is indicated as copies of mRNA per 1,000 copies of Actin-5c mRNA, and levels of miR-2 are indicated as copies per copy of U6. The different letters at the top of the columns in each histogram indicate statistically significant differences (in all cases $P \leq 0.05$), according to the REST software tool.

1. Belles X, Santos CG (2014) The MEKRE93 (Methoprene tolerant-Krüppel homolog 1-E93) pathway in the regulation of insect metamorphosis, and the homology of the pupal stage. *Insect Biochem Mol Biol* 52:60–68.

Table S1. Prediction of miRNA binding sites for miR-2, miR-13a, and miR13b in the 3′UTR of *B. germanica* Kr-h1 mRNA

Species	miRNA	3′UTR site	Rel. energy	Rel. score	Rel. total
B. germanica	miR-2	67	0.8	0.8	0.6
B. germanica	miR-13a	67	0.7	0.7	0.5
B. germanica	miR-13b	67	1.0	0.9	0.9
Pyrrhocoris apterus	miR-2	73	0.7	0.8	0.6
Rhodnius prolixus	miR-2	71	0.8	0.8	0.6
Acyrtosiphon pisum	miR-2	300	0.8	0.8	0.8

The sites were independently predicted by the following three algorithms: RNAhybrid (bibiserv.techfak.uni-bielefeld.de/rnahybrid/), used with a distribution probability of parameter $\xi = 1.98$ and $\Theta = 1.16$; miRanda (www.microrna.org/microrna/), with a score threshold of 100; and PITA (genie.weizmann.ac.il/index.html), with the seed limitation between 5 and 8. 3′UTR site indicates the first nucleotide where the miRNA seed region would bind, according to the mRNA sequence available in GenBank. To have a comparable quality estimator value among methods, the different scores are obtained by the normalization to 1 with reference to the best prediction. Rel. energy, the averaged relative value of energy; Rel. score, the relative value of scores; and Rel. total, the product Rel. energy × Rel. score.

Table S2. Forward (Fw) and reverse (Rv) primers used to measure mRNA and miRNA levels by qRT-PCR, to synthesize dsRNAs for RNAi, and to amplify the 3′UTR region of Kr-h1 mRNA: WT or to perform a site-directed mutagenesis suppressing the miR-2 site (Mut) for luciferase assays

Primers	5′–3′
qRT-PCR	
Kr-h1 Fw	GCGAGTATTGCAGCAAATCA
Kr-h1 Rv	GGGACGTTCTTTCGTATGGA
Met Fw	CTGTTGGGACATCAGCAGAA
Met Rv	GGCAGGTGATGGAGTGAAGT
BR-C Fw	CGGGTCGAAGGGAAAGACA
BR-C Rv	CTTGGCGCCGAATGCTGCGAT
E93 Fw	TCCAATGTTTGATCCTGCAA
E93 Rv	TTTGGGATGCAAAGAAATCC
Dicer-1 Fw	GCACTTGGGCACGAAAATCT
Dicer-1 Rv	ATCCAAAGGTGCCCATTCAA
Actin Fw	AGCTTCCTGATGGTCAGGTGA
Actin Rv	TGTCGGCAATTCCAGGGTACATGG
miR-2	TCACAGCCAGCTTTGATGA
miR-13a	TATCACAGCCACTTTGATGA
miR-13b	TATCACAGCCATTTTTGACGA
Let-7	TGAGGTAGTAGGTTGTATAGT
U6	CGATACAGAGAAGATTAGCATGG
dsRNA	
dsDicer-1 Fw	GGTGAGTCGGTTTGGTGAAT
dsDicer-1 Rv	CATGGCATGGCTAGGAATCT
dsKr-h1 Fw	GAATCTCAGTGTGCATAGGCG
dsKr-h1 Rv	CCTTGCCACAAATGACACAA
dsE93 Fw	AAAGAGTTGTCGGGAGCAGA
dsE93 Rv	GGAGTGGCTTCTAGCAGTGG
dsMock (Polyhedrin) Fw	ATCCTTTCCTGGGACCCGGCA
dsMock (Polyhedrin) Rv	ATGAAGGCTCGACGATCCTA
Vector luciferase	
Kr-h1 3′UTR WT Fw	GAGGAAGATTGATCTCACAG
Kr-h1 3′UTR WT Rv	TGAGTCATTTAATTTTTATT
Kr-h1 3′UTR Mut Fw	CCTCAAAAATGTAATGTGGTATTCTGGCC
Kr-h1 3′UTR Mut Rv	GGCCAGAATACCACATTACATTTTTGAGG